A Study of Shape and Polarization Fluctuations of a Water Droplet

Research Thesis

Presented in partial fulfillment of the requirements for graduation with research distinction in chemistry in the undergraduate colleges of The Ohio State University

By

Enda Xiao

The Ohio State University
April 2018

Project Advisor: Sherwin Singer, Department of Chemistry

A Study of Shape and Polarization Fluctuations of a Water Droplet

1 Introduction

While the properties of bulk fluids is of great interest, the behavior of fluids confined near surface or within finite regions, such as pores or droplets, is no less important. With regard to aqueous fluids, confined water is central to fields like geology, atmospheric science, aerosol science, and biology.

Confined water and aqueous solutions has been examined using various forms of spectroscopy, roughly falling into the ranges traditionally termed dielectric spectroscopy ($\nu \lesssim 10^{11} Hz$), terahertz spectroscopy ($10^{11} Hz \lesssim \nu \lesssim 10^{13} Hz$, or $3 cm^{-1} \lesssim h\nu \lesssim 300 cm^{-1}$), and vibrational spectroscopy ($100 cm^{-1} \lesssim h\nu \lesssim 5000 cm^{-1}$). Here, ν is the frequency of electromagnetic radiation and h is Planck's constant. In dielectric spectroscopy it is common to discuss the time scale

$$\tau = \frac{1}{2\pi\nu} = \frac{1}{\omega} \tag{1}$$

because absorption of electromagnetic radiation with angular frequency ω is associated with a physical process with time scale τ. An important feature in bulk water is the absorption peak variously reported with $\tau \approx$ 8.2-8.8ps,[1–3] known as the "Debye" peak associated with reorientation of water molecules.

In this work we study the shape and polarization fluctuations are a simple liquid water droplet in coexistence with water vapor, using both molecular dynamics simulations and analytic theory. Our main findings are that the Debye absorption feature is shifted to higher frequency by a factor of roughly 24, and that there is a weak coupling between shape and polarization fluctuations. To our knowledge, there are no experiments that directly test these calculations. We examined water droplets because it is an inherently interesting problem, it may hopefully motivate some experiments, and as a preparatory study to a possible investigation of more complex systems, like reserve micelles.

Reverse micelles are one of the most thoroughly studied systems by dielectric, terahertz, and vibrational spectroscopy. In reverse micelles Fig. 1, water droplets are stabilized within a non-aqueous solvent by a surfactant. Reverse micelles are convenient for study because the size of the droplets can be controlled by w, the number ratio of water to surfactant in the system.

$$w = \frac{[\text{water}]}{[\text{surfactant}]} \tag{2}$$

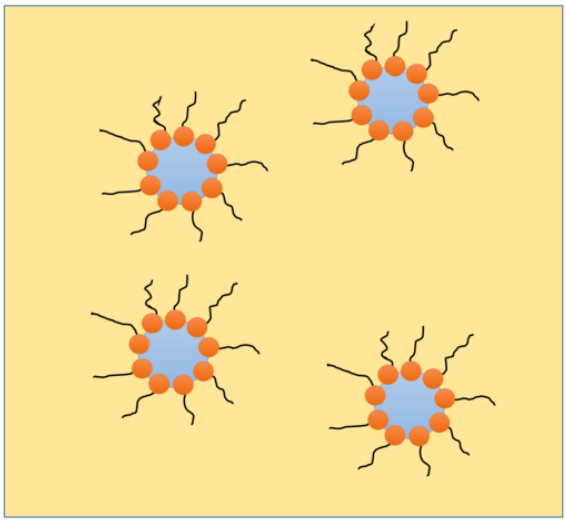

Figure 1: Schematic depiction of reverse micelles. Water is the color blue, and a non-aqueous solvent in which water is immiscible is a tan color. The polar or charged head groups of surfactants are arranged along the water surface, while the oily surfactant tails are within the outer solvent.

(In the literature, the ratio is called either w or w_0.) Assuming that the area density of surfactant does not change with droplet size, the water/surfactant ratio is the (droplet volume)/(droplet area) ratio, linearly dependent on droplet radius. Dielectric and terahertz spectroscopy reveal several qualitative features concerning reverse micelles.

- Spectral absorption feature with time scale that decreases from $\tau > 10ns$ for $w \lesssim 10$ to $\tau \sim 1ns$ for $w \gtrsim 10$.[4–7]
- The spectral absorption feature associated with Debye relaxation now appears at a higher frequency or shorter time scale, reported as $\tau \approx 5ps$,[7] $1ps$[8] and 2-$5ps$[9] for various surfactants and experimental conditions. In contrast to the lower frequency peak, the analogue of the Debye peak is either insensitive[7,8] or weakly dependent on w.

This paper consists of comparison of simple continuum theory for shape and dielectric fluctuations with detailed molecular simulations of water droplets. The document is organized as follows.

- Section 2: Details about molecular dynamics simulations of two droplets of 1728 and 13824 water molecules are provided.
- Section 3: We review available continuum theory that predicts shape fluctuations. The continuum theory is based on two ingredients. First, the energy change of the droplet as it fluctuates in shape is governed by the instantaneous surface area times the surface tension of the liquid. Second the motion of the fluid within its boundary is governed by linearized hydrodynamics. And the boundary condition that the radial velocity of the interface itself to equal radial velocity of both fluids at the interface is used. Continuum theory predicts that shape fluctuations for water clusters of the size for which we have performed molecular simulations should relax as an overdamped harmonic oscillator. We present evidence that our molecular simulations are in good agreement with continuum theory.

- Section 4: We consider a simple continuum theory for dielectric fluctuations of a spherical droplet, and predict the effect of confinement on the dielectric spectrum. Again, the continuum theory provides a good guide to the behavior of detailed molecular modeling.
- Section 5: We derive the high order coupling between shape and dielectric fluctuations within the context of continuum theory. These results are confirmed by molecular simulations.
- Section 6: We summarize our conclusions and discuss future applications in section .

2 Molecular dynamics simulations

We used the SPC/E interaction potential[10] was used to describe interactions between water models. The SPC/E model consists of three point charges at the hydrogen ($q_H = +0.4238e$) and oxygen ($q_O = -0.8476$) positions, plus a Lenndard-Jones potential between all oxygen pairs.

$$v(r) = 4\epsilon\left[\left(\frac{\sigma}{r}\right)^{12} - \left(\frac{\sigma}{r}\right)^{6}\right] \tag{3}$$

$$\sigma = 0.316556nm \tag{4}$$

$$\epsilon = 0.65017kJ\ mol^{-1} \tag{5}$$

Despite its simplicity, the SPC/E model yields a water density, diffusion constant and dielectric constant in good agreement with experiment.[11–13] Important properties of SPC/E water relevant to our work are given in Table

property	$T(K)$	SPC/E	experiment
dielectric constant ϵ	298	70.7[11]	78
surface tension	300	$6.13 \times 10^{-2} N/m$[13]	$7.28 \times 10^{-2} N/m$
density	300	$1.002 \times 10^{3} kg/m^{3}$[14]	$0.9965 \times 10^{3} kg/m^{3}$
kinematic viscosity	300	$7.02 \times 10^{-7} m^{2}/s$[14]	$8.56 \times 10^{-} m^{2}/s$

(6)

Table 1: Physical properties of the SPC/E model

3 Shape fluctuations

3.1 Decomposition of droplet shape in spherical harmonics

When gravitational effects are relatively small compared to interfacial tension effects, a droplet of water in equilibrium with vapor can be assumed to form a shape that slightly deviates from sphere. This droplet boundary as a function of solid angle Ω about a chosen droplet center can be depicted with spherical harmonics efficiently with few terms.[15,16]

$$r(\Omega) = r_0[1 + u(\Omega)] = r_0[1 + \sum_{\ell m} u_{\ell m} Y_{\ell m}(\Omega)] \tag{7}$$

The above form assumes that the droplet boundary function is single-valued in every direction from the droplet center, i.e. that no "overhangs" appear in its shape. From this expression, an expression for the volume and surface area of the droplet can be acquired.

A detailed derivation of the droplet volume and area in terms of the boundary function $r(\Omega)$ is provided in an appendix. Here we quote the relevant results. We can expand the third order term and ignore the high order terms because the $u_{\ell m}$ terms are small.

$$V = \frac{r_0^3}{3}\int \mathrm{d}\Omega \left(1 + \sum_{\ell,m} u_{\ell m} Y_{\ell,m}(\Omega)\right)^3 \tag{8}$$

$$= \frac{r_0^3}{3}\int \mathrm{d}\Omega \left[1 + 3\sum_{\ell,m} u_{\ell m} Y_{\ell,m}(\Omega) + 3\sum_{\ell,m}\sum_{\ell',m'} u_{\ell m} u^*_{\ell',m'} Y_{\ell,m}(\Omega) Y^*_{\ell',m'}(\Omega) + O(u^3)\right] \tag{9}$$

$$= \frac{4\pi r_0^3}{3}(1+u_0)^3 + r_0^3 \sum_{\ell>0,m} |u_{\ell m}|^2 + O(u^3), u_0 \equiv \frac{u_{00}}{\sqrt{4\pi}} \tag{10}$$

From this formula, one can obtain the required constraints on the and $u_{\ell m}$ to keep a constant volume $V = \frac{4\pi r_0^3}{3}$.

$$V = \frac{4\pi r_0^3}{3} = \frac{4\pi r_0^3}{3}(1+u_0)^3 + r_0^3 \sum_{\ell>0,m} |u_{\ell m}|^2 \tag{11}$$

$$(1+u_0)^3 = 1 - \frac{3}{4\pi}\sum_{\ell>0,m} |u_{\ell m}|^2 \text{ to maintain } V \text{ constant} \tag{12}$$

$$(1+u_0)^2 = (1 - \frac{3}{4\pi}\sum_{\ell>0,m} |u_{\ell m}|^2)^{\frac{2}{3}} \tag{13}$$

$$= 1 - \frac{1}{2\pi}\sum_{\ell>0,m} |u_{\ell m}|^2 + \ldots \tag{14}$$

The droplet area is given by the following expression.

$$A = \int \mathrm{d}A = \int \mathrm{d}\Omega \frac{r^2}{\hat{\boldsymbol{n}}\cdot\hat{\boldsymbol{r}}} \tag{15}$$

$$= \int \mathrm{d}\Omega \left(r^2 + \frac{r_0^2}{2}(u_\theta^2 + \frac{u_\phi^2}{\sin^2\theta})\right) \tag{16}$$

After integration,we have the expression for area.

$$A = \int \mathrm{d}\Omega \left(r^2 + \frac{r_0^2}{2}(u_\theta^2 + \frac{u_\phi^2}{\sin^2\theta})\right) \tag{17}$$

$$= 4\pi r_0^2(1+u_0)^2 + r_0^2 \sum_{\ell>0,m} |u_{\ell m}|^2 + \frac{r_0^2}{2}\sum_{\ell>0,m} \ell(\ell+1)|u_{\ell m}|^2 \tag{18}$$

$$= 4\pi r_0^2(1+u_0)^2 + r_0^2 \sum_{\ell>0,m} (1 + \frac{\ell(\ell+1)}{2})|u_{\ell m}|^2 \tag{19}$$

Then, we insert the relation that $(1+u_0)^2 = 1 - \frac{1}{2\pi}\sum_{\ell>0,m}|u_{\ell m}|^2 + \ldots$ into it to get the surface area at constant volume.

$$A = 4\pi r_0^2(1+u_0)^2 + r_0^2\sum_{\ell>0,m}(1+\frac{\ell(\ell+1)}{2})|u_{\ell m}|^2 \tag{20}$$

$$= 4\pi r_0^2(1-\frac{1}{2\pi}\sum_{\ell>0,m}|u_{\ell m}|^2) + r_0^2\sum_{\ell>0,m}(1+\frac{\ell(\ell+1)}{2})|u_{\ell m}|^2 \tag{21}$$

$$= 4\pi r_0^2 + \frac{r_0^2}{2}\sum_{\ell>0,m}(\ell+2)(\ell-1)|u_{\ell m}|^2 \tag{22}$$

This is the expression of area of a droplet with constant volume, later used to estimate the surface energy of the fluctuating droplet.

3.2 Analytical treatment of the damped droplet decay

The shape fluctuation of a droplet in fluid medium is well studied by A. Prosperetti,[17,18] and by C. A. Miller and L. E. Scriven.[19] In Miller and Scriven's paper, the droplet is assumed to be isothermal, incompressible, and Newtonian. The ratio of radial displacement of the surface to the wavelength along the surface is assumed to be small, so that the nonlinear term in the Navier-Stokes equation can be neglected. This reasonable assumption can make the motion equation much simper. The resulting equation for the flow velocity field $\mathbf{v}(\mathbf{r})$ is known as the Stokes equation.

$$\frac{\partial \mathbf{v}}{\partial t} = -\frac{1}{\rho}\nabla P + \nu\nabla^2\mathbf{v} \tag{23}$$

In the above equation, P is the pressure, ρ is the mass density, and ν is the shear viscosity. The Stokes equation is solved with the boundary condition that component of $\mathbf{v}(\mathbf{r})$ normal to the droplet boundary is zero. It is convenient to introduce an auxiliary function, the vorticity.

$$\mathbf{w}(\mathbf{r}) = \boldsymbol{\nabla}\times\mathbf{v}(r) \tag{24}$$

The radial components of $\mathbf{v}(\mathbf{r})$ and $\mathbf{w}(\mathbf{r})$, $v(r)$ and $w(r)$, respectively, satisfy the following differential equations.

$$\nabla^2(\frac{\partial}{\partial t} - \nu\nabla^2)(rw(r)) = 0 \tag{25}$$

$$(\frac{\partial}{\partial t} - \nu\nabla^2)(rv(r)) = 0 \tag{26}$$

It is supposed that $v(r)$ and $w(r)$ can be expanded in terms of spherical harmonics.

$$rv(r) = e^{-\beta_l t}V_{lm}(r)Y_l^m(\Omega) \tag{27}$$

$$rw(r) = e^{-\beta_l t}W_{lm}(r)Y_l^m(\Omega) \tag{28}$$

In the above equation, β_l is the time constant that describes how a distortion of tensor rank l decays to zero. In general, β_l will solve a quadratic equation. The two roots will either be complex

conjugate pairs of complex numbers, the under-damped case, or two real roots, the over-damped case. Our systems falls in the over-damped regime. The smaller of the two roots for β_l gives the long-time approach to equilibrium.

When droplet and outer fluid is separated by a clean and simple interface which makes coefficients of interfacial viscosity and elasticity to be zero, β_l is obtained by setting the following determinant equal to zero,

$$\begin{vmatrix} \beta_l & 1 & 0 & 0 & 0 \\ 0 & 1 & 0 & -1 & 0 \\ 0 & 1-l & w_i R Q^J_{l+\frac{1}{2}} & -(l+2) & C(H) \\ \frac{-\beta_l^{\star 2}\Gamma}{l(l+1)} & \frac{\beta_l \rho_i}{l} - \frac{2(l-1)\mu_i}{R^2} & \frac{2\mu_i w_i}{R} Q^J_{l+\frac{1}{2}} - \frac{\beta_l \rho_i}{l} & \frac{\beta_l \rho_0}{l+1} - \frac{2\mu_0(l+2)}{R^2} & \frac{-\beta_l \rho_o}{l+1} + \frac{2\mu_0}{R^2} C(H) \\ 0 & 2\mu_i(l^2-1) & \mu_i G(J) & -2\mu_o l(l+2) & \mu - 0F(H) \end{vmatrix} = 0\,, \tag{29}$$

where

$$\begin{aligned} Q^J_{l+1/2} &= \frac{J_{l+3/2}(w_i R)}{J_{l+1/2}(w_i R)} \\ C(H) &= 2l + 1 - w_o R Q^H_{l+\frac{1}{2}} \\ F(H) &= 2(2l+1) + w_0^2 R^2 - 2w_0 R Q^H_{l+\frac{1}{2}} \\ \Gamma &= \rho_o l + \rho_i (l+1) \\ \rho_{i/o} &= \text{inner/outer fluid density} \\ J_{l+1/2} &= \text{half-integral-order Bessel function} \\ w_i &= \sqrt{\frac{\beta_l}{\nu}} \\ R &= \text{radius of droplet} \\ \mu_{i/o} &= \text{inner/outer fluid dynamic viscosity} \end{aligned}$$

3.3 Result of continuum theory

In Miller and Scriven's work, they provide much simplified versions of this equation at different cases with proper approximations. The equation in the case that exterior fluid is rarefied and its effect on the motion of droplet is negligible is a proper one used to determine the frequency of droplet in vacuum analytically.

$$\frac{\beta_l^{\star 2}}{\beta_l^2} = \frac{2(l^2-1)}{w_i^2 R^2 - 2w_i R Q^J_{l+1/2}} - 1 + \frac{2l(l-1)}{w_i^2 R^2}[1 - \frac{(l+1)Q^J_{l+1/2}}{\frac{1}{2}w_i R - Q^J_{l+1/2}}] \tag{30}$$

where

$$
\begin{aligned}
Q^J_{l+1/2} &= \frac{J_{l+3/2}(w_i R)}{J_{l+1/2}(w_i R)} \\
\beta^\star_l &= \left(\frac{\gamma l(l+1)(l-1)(l+2)}{R^3\Gamma}\right)^{\frac{1}{2}} \\
\Gamma &= \rho_o l + \rho_i (l+1) \\
J_{l+1/2} &= \text{half-integral-order Bessel function} \\
w_i &= \sqrt{\frac{\beta_l}{\nu}} \\
R &= \text{radius of droplet} \\
\rho_{i/o} &= \text{inner/outer fluid density}
\end{aligned}
$$

3.4 Compare shape decay frequencies obtained by MD and continuum theory

According to linear response theory,[20,21] the decay of a weak perturbation from equilibrium should decay as the time correlation function of the disturbance. Therefore, the solution of Eq. (30) for β_l gives the time constant for a correlation function of a tensor of rank l to decay to its long-time value. Since they are linear combinations of spherical tensor elements Y_{2m}, the elements of the following Cartesian tensor should decay to zero with time constant β_2.

$$
G_{ab}(t) = \frac{\langle \overline{r_a r_b}(t)\overline{r_a r_b}(0)\rangle - \langle \overline{r_a r_b}\rangle^2}{\langle \overline{r_a r_b}(0)\overline{r_a r_b}(0)\rangle} = e^{-\beta_2 t} \qquad a, b = x, y, z \tag{31}
$$

In the above equation, the overbars indicate average over molecules in the droplet,

$$
\overline{r_a r_b}(t) = \frac{1}{N}\sum_{i=1}^{N}\sum_{j=1}^{N} r_{ia} r_{jb}\,, \tag{32}
$$

where r_{ia} is the ath Cartesian component of oxygen i from the center of mass of the droplet. The angle brackets indicate a time average required to accumulate a correlation function over a simulation of duration T.

$$
\langle A(t)B(0)\rangle \approx \frac{1}{(T-t)}\int_0^{T-t} dt' A(t'+t)B(t') \tag{33}
$$

All the elements of the tensor $\mathbf{G}$ should decay with decay constant β_2. In practice, we accumulated the average diagonal element of the tensor $\mathbf{G}(t)$, that is, one-third of the trace of $\mathbf{G}(t)$.

$$
\frac{1}{3}\mathrm{Tr}\left[\mathbf{G}(t)\right] = \frac{1}{3}\left[G_{xx}(t) + G_{yy}(t) + G_{zz}(t)\right] \tag{34}
$$

Averaging three elements gives us better statistics. The results are shown in Fig. 2, along with exponential fits.

The decay constant for decay of shape fluctuations calculated using equation (30) is compared with molecular dynamics results in Table 2. Continuum theory provide an excellent description of droplet shape fluctuations.

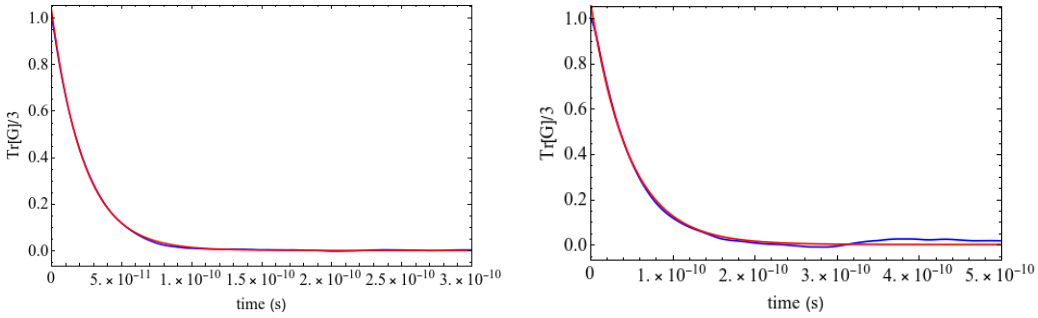

Figure 2: The shape fluctuation correlation function, $\frac{1}{3}\mathrm{Tr}\,[\mathbf{G}(t)]$ [Eq. (34)] for water droplets consisting of 1728 (left) and 13824 (right) molecules. The molecular dynamics results are the blue curves, and the exponential fit is in red.

Table 2: Decay constants for droplet shape fluctuations

	1728 water	13824 water
simulation β (Hz)	4.34335×10^{10}	2.13338×10^{10}
analytic β (Hz)	4.15456×10^{10}	2.17637×10^{10}

4 Dielectric fluctuations

4.1 Polarization in bulk and in finite systems with interfaces

4.1.1 bulk system without boundaries

An electric field is applied to bulky material induces a polarization. In a homogeneous system, polarization is the dipole moment per unit volume. When the system is inhomogeneous, as in the case with boundaries, the notion of polarization has to be generalized, as described later. At the level of continuum theory, polarization fluctuations in the presence of an electric field are governed by the following Hamiltonian.

$$H = \int_V d\mathbf{r} \left[\frac{\mathbf{P}^2}{2\epsilon_0(\epsilon - 1)} - \mathbf{E} \cdot \mathbf{P} \right] \tag{35}$$

The first term on the right hand side represents the free energy cost of aligning polar molecules. The second term is the energy gain when dipoles align with the field.

The minimum free energy polarization is obtained by minimizing H, leading to the familiar result,

$$\mathbf{P} = \epsilon_0(\epsilon - 1)\mathbf{E}\,. \tag{36}$$

The factor $(\epsilon - 1)$ is the electric susceptibility χ.

$$\chi = \epsilon - 1 \tag{37}$$

4.1.2 slab

When uniform electric filed is applied to the the material confined within infinite slabs, the condition is different from the bulk material condition. The induced polarization within the material

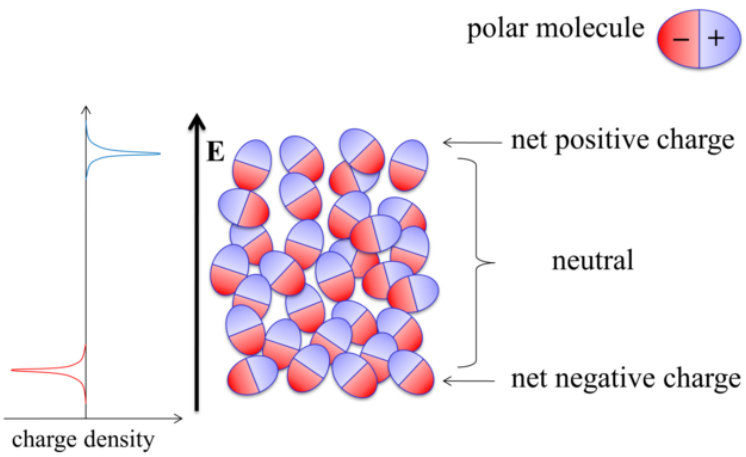

Figure 3: Origin of polarization charge within an infinite slab.

induces surface charge on the boundary of the surface (Fig. 3).[22] In continuum theory, the magnitude of the polarization charge is $\mathbf{n} \cdot \mathbf{P}$, where $\mathbf{P}$ is the polarization in the interior of the sample and $\mathbf{n}$ is the outward surface normal. Thus, an extra term corresponding to the Coulumb potential between boundary charges, repulsive between like charges on the same surface and attractive between charges on opposite surfaces, should be added into the expression of the total energy. A detailed derivation is provided in the appendix. The result is a net increased free energy cost $\frac{1}{2\epsilon_0}\mathbf{P}^2$ that must be added to the bulk Hamiltonian of Eq. (35).

$$H = \int_V d\mathbf{r} \left[\frac{\mathbf{P}^2}{2\epsilon_0(\epsilon - 1)} - \mathbf{E}_0 \cdot \mathbf{P} + \frac{1}{2\epsilon_0}\mathbf{P}^2 \right] = \int_V d\mathbf{r} \left[\frac{\epsilon \mathbf{P}^2}{2\epsilon_0(\epsilon - 1)} - \mathbf{E}_0 \cdot \mathbf{P} \right] \tag{38}$$

The polarization in the uniform electric field is reduced by a factor of ϵ compared to the bulk.

$$\mathbf{P} = \epsilon_0 \left(1 - \frac{1}{\epsilon} \right) \mathbf{E}_0 \tag{39}$$

We use the symbol $\mathbf{E}_0$ for the applied field as a reminder that the total field within the material is reduced by the polarization charge at the surface,

$$\mathbf{E} = \frac{1}{\epsilon}\mathbf{E}_0 \tag{40}$$

4.1.3 sphere

When the electric field is applied to a spherical droplet, we must again account for the Coulomb potential arising from polarization charge (Fig. 4). The detailed derivation of total energy is provided in the appendix. The result is an additional cost of polarization equal to $\frac{1}{6\epsilon_0}\mathbf{P}^2$.

$$H = \int_V d\mathbf{r} \left[\frac{\mathbf{P}^2}{2\epsilon_0(\epsilon - 1)} - \mathbf{E}_0 \cdot \mathbf{P} + \frac{1}{6\epsilon_0}\mathbf{P}^2 \right] = \int_V d\mathbf{r} \left[\frac{(\epsilon + 2)}{6\epsilon_0(\epsilon - 1)\mathbf{P}^2} - \mathbf{E}_0 \cdot \mathbf{P} \right] \tag{41}$$

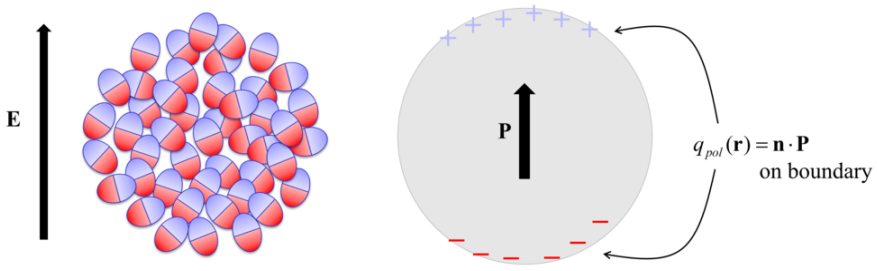

Figure 4: Origin of polarization charge within a spherical drop.

The polarization of droplet in the electric field is

$$\mathbf{P} = \epsilon_0 \frac{3(\epsilon - 1)}{\epsilon + 2})\mathbf{E}_0 \,, \tag{42}$$

a well known result for a dielectric sphere.

4.2 The frequency dependent susceptibility

In the previous sections, we considered polarization of a bulk material, a slab, and a sphere in response to a static field $\mathbf{E}$. We found that $\mathbf{P} = \epsilon_0 \chi \mathbf{E} = \epsilon_0(\epsilon - 1)\mathbf{E}$ depends on the system geometry. Next we consider linear response to a time-dependent field. It is useful to examine a single frequency component.

$$\mathbf{E}(t) = \mathbf{E}(\omega)e^{i\omega t} \tag{43}$$

Of course, complex-valued fields are not available in the lab. However any real experimental field can be synthesized as a linear combination of pure frequency components. For example, a field that is proportional to $\cos \omega t$ is a superposition of pure frequency components ω and $-\omega$.

Standard results of linear response theory[21,23] tell us that a perturbation of frequency ω produces a polarization with the same frequency.

$$\mathbf{P}(\omega) = \epsilon_0 \boldsymbol{\chi}(\omega)\mathbf{E}(\omega) = \epsilon_0(\boldsymbol{\epsilon} - \mathbf{1})\mathbf{E}(\omega) \tag{44}$$

In general, $\boldsymbol{\chi}(\omega)$ is a 3×3 susceptibility tensor. When the system is isotropic and non-crystalline, $\boldsymbol{\chi}(\omega)$ is diagonal and all three diagonal elements are identical.

Linear response theory tells us that susceptibilities can be expressed in terms of time correlation functions evaluated in the absence of the perturbing fields. The electrical susceptibility $\boldsymbol{\chi}(\omega)$ is given in many forms, one of which is in terms of time correlation functions of the total system dipole $\mathbf{M}(t) = \sum_{i=1}^{N} q_i \mathbf{r}_i(t)$.

$$\boldsymbol{\chi}(\omega) = \frac{\beta}{\epsilon_0 V}\left[\langle \mathbf{MM} \rangle + i\omega \int_0^\infty dt\, e^{i\omega t} \langle \mathbf{M}(t)\mathbf{M}(0) \rangle\right] \,, \tag{45}$$

In general, $\boldsymbol{\chi}(\omega)$ is complex-valued. We can write,

$$\boldsymbol{\chi}(\omega) = \boldsymbol{\chi}'(\omega) + i\boldsymbol{\chi}''(\omega) \,. \tag{46}$$

The imaginary part of the susceptibility measures the rate at which the system absorbs energy from the perturbing field. $\chi''(\omega)$ is the absorption spectrum.

When the dipole-dipole correlation function decays exponentially,

$$\langle \mathbf{M}(t)\mathbf{M}(0)\rangle = \langle \mathbf{M}(0)\mathbf{M}(0)\rangle\, e^{-t/\tau}\,, \tag{47}$$

the diagonal elements of the susceptibility tensor are given as follows.

$$\chi(\omega) = \chi'(\omega) + i\chi''(\omega) \tag{48}$$

$$\epsilon(\omega) - 1 = \epsilon'(\omega) - 1 + \epsilon''(\omega) \tag{49}$$

$$\chi'(\omega) = \epsilon'(\omega) - 1 = (\epsilon - 1)\frac{1}{1 + (\omega\tau)^2} \tag{50}$$

$$\chi''(\omega) = \epsilon''(\omega) - 1 = (\epsilon - 1)\frac{\omega\tau}{1 + (\omega\tau)^2} \tag{51}$$

In the equations above, ϵ is the static dielectric constant. The behavior of $\chi'(\omega)$ and $\chi''(\omega)$ with exponential relaxation of $\langle \mathbf{M}(t)\mathbf{M}(0)\rangle$ are shown in Fig. 5.

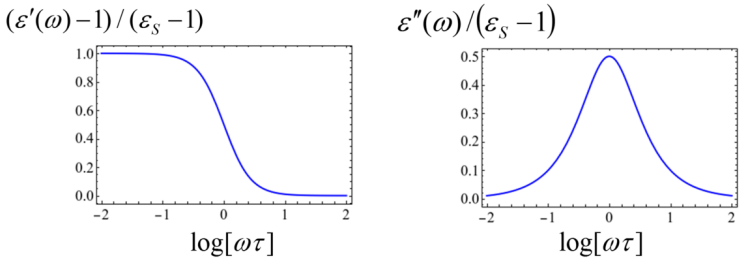

Figure 5: Behavior of $\chi'(\omega)$ and $\chi''(\omega)$ with exponential relaxation of $\langle \mathbf{M}(t)\mathbf{M}(0)\rangle$

4.3 Debye peak shifted in confined configuration based on the continuum Hamiltonian, compared with MD

A damped oscillation mode can be used to depict the polarization fluctuation. To make the math easy and familiar, we recall Newton's equation for a damped harmonic oscillator.

$$m\ddot{x} = -kx - \beta\dot{x} \tag{52}$$

where m is mass of the spring, k is the spring constant and β is the friction constant. When we rearrange all terms to the left side, then insert the general solution that $x = x_0 e^{-\zeta t}$ and eliminate the shared and nonzero exponential term on both sides. This leads to the following secular equation.

$$m\zeta^2 + \beta\zeta + k = 0 \tag{53}$$

$$\zeta^2 + 2\gamma\zeta + \omega_0^2 = 0 \quad \text{where} \quad 2\gamma = \frac{\beta}{m} \quad \omega_0^2 = \frac{k}{m} \tag{54}$$

The eigenfrequencies that emerge from the secular equation are

$$\zeta = \gamma \pm \sqrt{\gamma^2 - \omega_0^2} \tag{55}$$

$$= \gamma \pm \gamma \sqrt{1 - \left(\frac{\omega_0}{\gamma}\right)^2} \tag{56}$$

$$\tag{57}$$

Since the polarization fluctuations are heavily overdamped, $\frac{\omega_0}{\gamma}$ is very small. The square root can be expanded in terms of $\frac{\omega_0}{\gamma}$.

$$\zeta = \gamma \pm \gamma(1 - \frac{1}{2}\frac{\omega_0^2}{\gamma^2} + ...) \tag{58}$$

$$= \left\{ \begin{array}{ll} 2\gamma - \frac{\omega_0^2}{2\gamma} + \cdots \equiv \zeta_f & \text{fast decay.} \\ \frac{\omega_0^2}{2\gamma} + \cdots \equiv \zeta_s & \text{slow decay} \end{array} \right\} \tag{59}$$

The trajectory of the damped harmonic oscillator in the overdamped limit can be written as

$$x(t) = x_f(0)e^{-\zeta_f t} + x_s(0)e^{-\zeta_s t} \tag{60}$$

Since $\gamma >> \frac{\omega_0^2}{\gamma}$, the fast component rapidly decays to zero. After a short time,

$$x(t) \approx x_s(0)e^{-\zeta_s t}, \zeta_s = \frac{\omega_0^2}{2\gamma} \qquad \text{when } t >> \frac{1}{2\gamma} \tag{61}$$

and the coordinate decays to zero as a single exponential. The decay rate increases with the force constant of the harmonic oscillator ($\zeta_s \propto \omega_0^2$), and decreases with the friction ($\zeta_s \propto 1/\gamma$).

We now consider polarization fluctuations as a damped harmonic oscillator and ask how polarization fluctuations should decay in a spherical droplet compared the bulk. Recall from Eq. (47), that in a simple Debye model, polarization fluctuations decay with time scale τ. Making the analogy with the damped harmonic oscillator, we would expect τ in Eq. (47) to scale inversely to the coefficient of $\mathbf{P}^2$ in the polarization Hamiltonians, Eqs. (35) (bulk), (38) (slab) or (41) (sphere). For simplicity we assume that the friction coefficient is the same for the droplet and bulk.

$$\frac{\tau_{\text{bulk}}}{\tau_{\text{sphere}}} = \frac{\omega_{0,\text{sphere}}^2}{\omega_{0,\text{bulk}}^2} = \frac{(\epsilon + 2)\,(3(\epsilon - 1))^{-1}}{(\epsilon - 1)^{-1}} = \frac{\epsilon + 2}{3} \tag{62}$$

Our expectation is that polarization fluctuations for SPC/E water at $300K$ should decay faster in the droplet compared to the bulk by the factor

$$\frac{\tau_{\text{bulk}}}{\tau_{\text{sphere}}} \approx \frac{70.7 + 2}{3} = 24.2\,, \tag{63}$$

and that the effect should be independent of droplet size.

This ratio is qualitatively, not quantitatively confirmed by simulation result of the bulk water and water clusters of two different size. The dielectric spectra of the bulk water and water droplet

are displayed below in Figs. 6 and 7. The peak at about $10^{11} Hz$ in the bulk water spectrum is called Debye peak which is corresponding to the polarization decay.

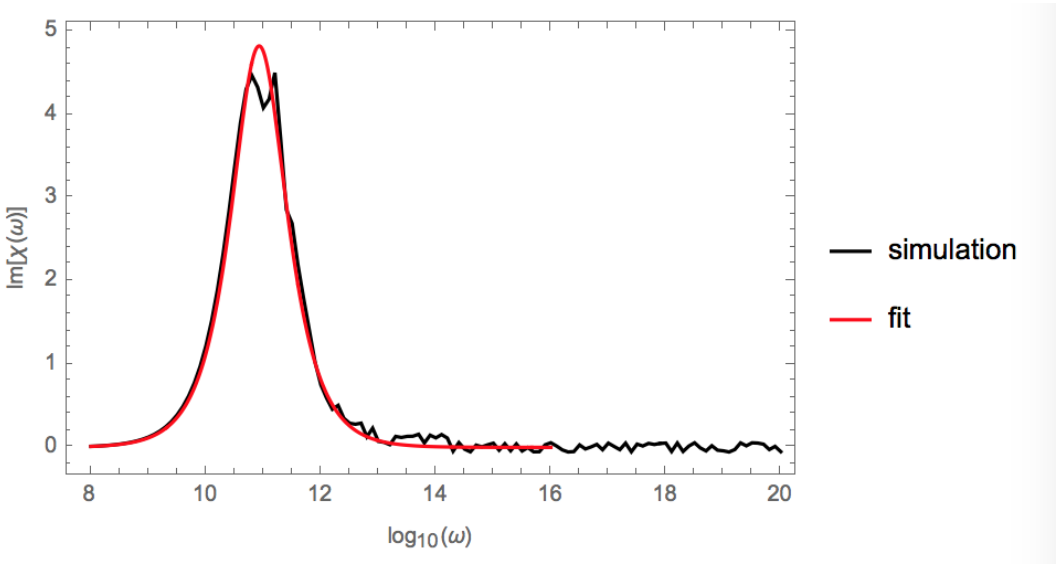

Figure 6: Dielectric Spectrum of bulk water (imaginary part)

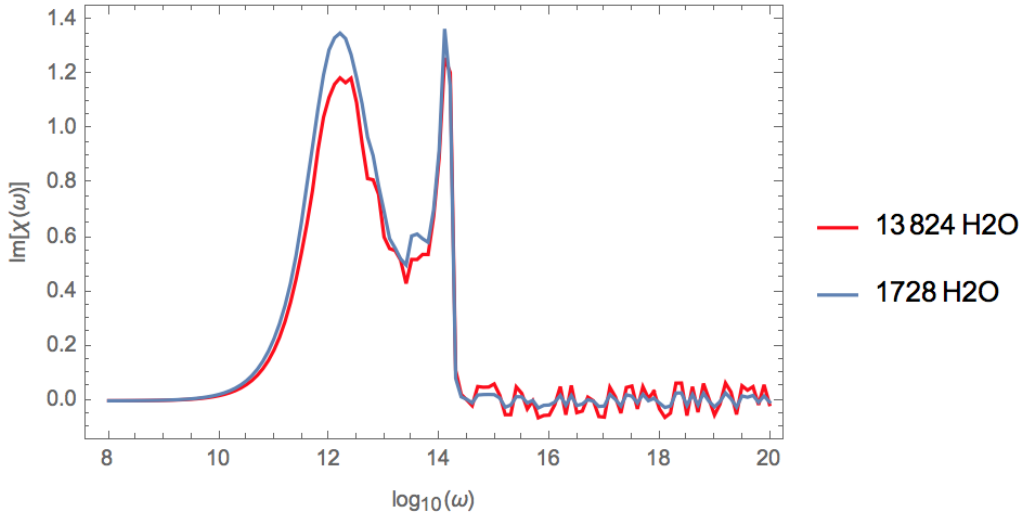

Figure 7: Dielectric Spectrum of two different size clusters (imaginary part)

The peaks of two droplets are at almost the same frequencies, matching with the prediction the frequency of the water droplet is independent of the size. The frequency of peaks are determined by fitting to the formula of the Debye relaxation $\chi(\omega) = \frac{\omega\tau_D}{1+(\omega\tau_D)^2}$. The result are display in the table below.

Table 3: The frequency of Debye peaks of bulk water and water clusters

	$\log_{10}(\omega)$	ω	ratio to bulk water
bulk water	10.98	9.508×10^{10}	1
1728 water molecules	12.22	1.660×10^{12}	17.45
13824 water molecules	12.24	1.738×10^{12}	18.28

The ratio obtained using simulation is large, but not quite as large as the prediction. At this point, it is not clear why simulation and analytic theory do not match better. One possible reason is that the prediction of continuum theory assumes that the layer of polarization charge is infinitesimally thin. It is actually distributed over a layer up to $1nm$ in thickness.[22] Another reason may lie with the fact that the dipole-dipole correlation function of the droplets is not a single exponential. $\ln\left[\langle \mathbf{M}(t) \cdot \mathbf{M}(0)\rangle /3\right]$ for the small cluster (1728 molecules) is shown in Fig. 8. The correlation

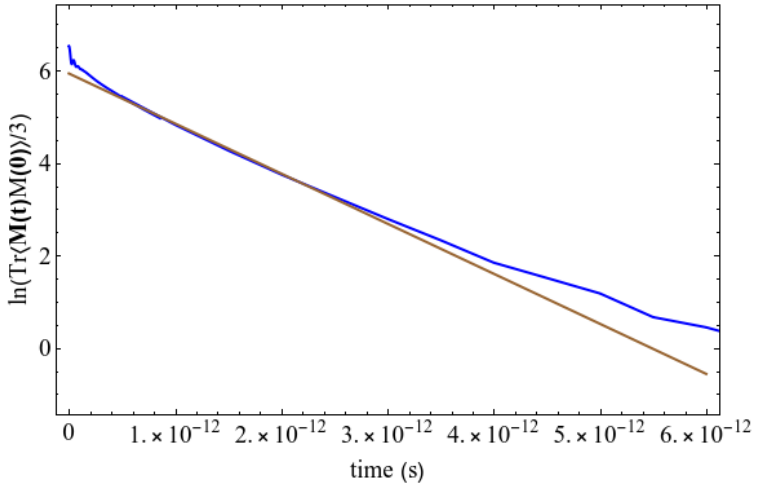

Figure 8: $\ln\left[\left\langle M_x(t)M_x(0) + M_y(t)M_y(0) + M_z(t)M_z(0)\right\rangle /3\right] = \ln\left[\mathrm{Tr}\,\langle \mathbf{M}(t) \cdot \mathbf{M}(0)\rangle /3\right]$ for a cluster of 1728 water molecules (blue curve). The brown line is shown to demonstrate that the correlation function departs from a single exponential.

function is juxtaposed against a straight line to confirm that the correlation function is nowhere exponential.

The deviation from exponential at times less than $1ps$ is expected. It is the well-understood "inertial" behavior.[24–26] However, the decay departs from exponential at later times as well. Explaining this departure is an unfinished part of this research. We do have a hypothesis: Shape fluctuations (30-50ps,Table 2) are much slower than polarization fluctuations (0.6ps, Table 3). Therefore, polarization fluctuations take place in a cluster that can be regarded as statically distorted. In the next section, we show that polarization fluctuations are coupled to shape fluctuations. They are slightly slower along a long axis, like the long axis of a prolate body, and faster along a short axis, like the short axes of a prolate body. As a result, the Debye peak of a cluster is really three peaks, corresponding to the three principle axes of the cluster, averages over shape fluctuations. This may explain the non-exponential behavior.

5 Coupled relationship between shape and polarization

5.1 Derivation of the coupling relationship between shape and polarization

When the droplet is allowed to deform, the total energy of the droplet in continuum theory is more complicated than the fixed configurations such as slab or sphere. The deformed shape influences the surface energy because the total surface area changes upon distortion (with volume fixed), and the Coulumb potential due to the change in polarization charge, $(n)\cdot\mathbf{P}$ along the deformed surface. To calculate the polarization energy, we borrowed from the literature on magnetic polarization.[27,28] The Coulomb energy cost of forming polarization charge is expressed in terms of the Fourier transform of the polarization density.

$$u_{pol} = \frac{1}{2}\int_V d\mathbf{r}_1 \int_V d\mathbf{r}_2 \frac{q_{pol}(\mathbf{r}_1)\, q_{pol}(xs\mathbf{r}_2)}{4\pi\epsilon_0|\mathbf{r}_1-\mathbf{r}_2|} = \frac{1}{(2\pi)^2 4\pi\epsilon_0}\int d\mathbf{k}\,|\hat{\mathbf{k}}\cdot\mathbf{P}(\mathbf{k})|^2 \tag{64}$$

$$\text{where } \mathbf{P}(\mathbf{k}) = \int_V d\mathbf{r} e^{-i\mathbf{k}\cdot\mathbf{r}}\mathbf{P}\,, \qquad \hat{\mathbf{k}} = \frac{\mathbf{k}}{|\mathbf{k}|}\,, \tag{65}$$

and the distorted shape enter through the integral limits of the $\mathbf{r}$-space integration over the droplet volume V. The integral over $\mathbf{k}$ is over all of $\mathbf{k}$-space.

In continuum theory, the total energy is composed of three contributions. γA is the cost of forming the droplet surface with area A, u_{EP} is the interaction between the applied field and the polarization, and u_{pol} is the energetic cost of generating polarization charge [Eq. (64)].

$$H = \gamma A + u_{EP} + u_{pol} \tag{66}$$

$$= \gamma\left(4\pi r_0^2 + \frac{r_0^2}{2}\sum_{l>0,m}(l+2)(l-1)|u_{lm}|^2\right) + \frac{4\pi r_0^3}{3\epsilon_0}\left[-\mathbf{E}_0\cdot\mathbf{P} + \frac{\mathbf{P}^2}{2}\left(\frac{\epsilon+2}{3(\epsilon-1)} - \frac{1}{\sqrt{5\pi}}u_{20} + ...\right)\right] \tag{67}$$

The leading term in shape distortion-polarization coupling is the one proportional to $\mathbf{P}^2 u_{20}$, where the angles in the spherical harmonic expansion are with respect to the polarization vector $\mathbf{P}$.

From this we learn that to quadratic order, there is no shape distortion-polarization coupling. The leading term is

$$\propto -|\mathbf{P}|^2 u_{20}\,, \tag{68}$$

where u_{20} is the coefficient of the spherical harmonics Y_2^0. The expansion $r(\Omega) = r_0(1 + u_{lm}Y_l^m(\Omega))$ is referred to the direction of $\mathbf{P}$. A larger u_{20} value suggests a more elongated shape. Thus, this term suggests that polarizations along the elongated direction/distortion along $\mathbf{P}$ are favored.

5.2 Polarization in body frame

The moment of inertia tensor of the 1728 water droplet is calculated for each frame of the simulation. Then the moment of inertia tensor is diagonalized to find the principle axis direction of the droplet. The principle directions of droplet is also the directions along which the droplet elongates or compresses. The polarization along these directions are calculated and the results are displayed in the table below.

The polarization value is largest in the elongated direction. It conforms the derivation conclusion that the polarization and the shape fluctuation are coupled. The polarization along the elongated direction is favored.

Table 4: Polarization along the principle axes (elongated or shortened axes)

direction	Polarization square $\langle M^2 \rangle$
most elongated	737.97 $Debye^2$
second	682.03 $Debye^2$
third	633.284 $Debye^2$

6 Conclusion

From this exercise, we have learned that continuum models have significant predictive power in describing polarization and shape fluctuations of a water droplet, and the coupling between shape and polarization fluctuations. In particular, shape fluctuations match continuum predictions nearly quantitatively. Two aspects of polarization fluctuations in a droplet agree with continuum predictions: droplet polarization fluctuations occur on a much faster time scale, and this shift is independent of droplet size. The magnitude by which droplet polarization fluctuations are sped up is 70-75% of continuum predictions. We advanced two reasons for this quantitative discrepancy: The droplet dielectric spectrum must be re-analyzed taking droplet shape distortion into account, and the fact that in the droplet the polarization charge is distributed over a finite volume, and is not concentrated in an infinitesimally thin layer as assumed in continuum theory.

Several tasks lay ahead to wrap up this work.

- Statistical error bars must be generated for the simulation data
- Using analytic theory, we should test the notion that allowing the polarization charge to be spread over a finite volume in continuum theory will improve the comparison between continuum theory and molecular dynamics.
- The comparison of analytic theory and simulation with respect to coupling of polarization and shape fluctuations should be more quantitative.

It is tantalizing to speculate that what has be learned about isolated water droplet fluctuations is relevant to the observed dielectric spectrum of reverse micelles, which contain pools of water confined by a surfactant layer and non-polar solvent. We are considering whether to attempt a simulation of a reverse micelle in order to confirm these speculations.

References

[1] J. B. Hasted. Liquid water: Dielectric properties. In F. Franks, editor, *Water: A Comprehensive Treatise*, volume 1, pages 255–309. Plenum, New York, 1972.

[2] J. Barthel, K. Bachhuber, R. Buchner, and H. Hetzenauer. Dielectric spectra of some common solvents in the microwave region. water and lower alcohols. *Chem. Phys. Lett.*, 165(4):369–373, 1990.

[3] J. T. Kindt and C. A. Schmuttenmaer. Far-infrared dielectric properties of polar liquids probed by femtosecond terahertz pulse spectroscopy. *J. Phys. Chem.*, 100(24):10373–10379, 1996.

[4] M. A. Van Dijk, C. C. Boog, G. Casteleijn, and Y. K. Levine. Time domain spectroscopic dielectric permittivity measurements on aot/water/isooctane. *Chem. Phys. Lett.*, 111(6):571–573, 1984.

[5] R. Henze and U. Schreiber. Dielectric relaxation measurements on aerosol-OT/water/cyclohexane-solutions at low water content. *Colloid Polym. Sci.*, 263(2):164–172, 1985.

[6] G. Onori and A. Santucci. Hydration and dynamics of aerosol ot microemulsions: infrared and microwave dielectric spectroscopy. *Trends in Chemical Physics*, 4:215–225, 1996.

[7] M. D'Angelo, D. Fioretto, G. Onori, L. Palmieri, and A. Santucci. Study of the dynamics of water/aerosol ot/n-heptane system by dielectric relaxation measurements. *Colloid Polym. Sci.*, 273(9):899–905, 1995.

[8] Daniel M. Mittleman, Martin C. Nuss, and Vicki L. Colvin. Terahertz spectroscopy of water in inverse micelles. *Chem. Phys. Lett.*, 275(3,4):332–338, 1997.

[9] Animesh Patra, Trung Quan Luong, Rajib Kumar Mitra, and Martina. Havenith. The influence of charge on the structure and dynamics of water encapsulated in reverse micelles. *Phys. Chem. Chem. Phys.*, 16(25):12875–12883, 2014.

[10] H. J. C. Berendsen, J. R. Grigera, and T. P. Straatsma. The missing term in effective pair potentials. *J. Phys. Chem.*, 91(24):6269–6271, 1987.

[11] M. Rami Reddy and M. Berkowitz. The dielectric constant of spc/e water. *Chem. Phys. Lett.*, 155(2):173–176, 1989.

[12] S. Balasubramanian, Christopher J. Mundy, and Michael L. Klein. Shear viscosity of polar fluids: Molecular dynamics calculations of water. *J. Chem. Phys.*, 105(24):11190–11195, 1996.

[13] Feng Chen and Paul E. Smith. Simulated surface tensions of common water models. *J. Chem. Phys.*, 126(22):221101, 2007.

[14] Paul E. Smith and Wilfred F. van Gunsteren. The viscosity of SPC and SPC/E water at 277 and 300 K. *Chem. Phys. Lett.*, 215(4):315–318, 1993.

[15] Stig Ljunggren and Jan Christer Eriksson. Shape fluctuations of spherical micelles. *J. Chem. Soc., Faraday Trans. 2*, 80(4):489–497, 1984.

[16] S. T. Milner and S. A. Safran. Dynamic fluctuations of droplet microemulsions and vesicles. *Phys. Rev. A*, 36(9):4371–4379, 1987.

[17] Andrea Prosperetti. Free oscillations of drops and bubbles - the initial-value problem. *J. Fluid Mech.*, 100:333–347, 1980.

[18] A. Prosperetti. Normal-mode analysis for the oscillations of a viscous-liquid drop in an immiscible liquid. *Journal De Mécanique*, 19(1):149–182, 1980.

[19] C. A. Miller and L. E. Scriven. The oscillations of a fluid droplet immersed in another fluid. *J. Fluid Mech.*, 32(3):417–435, 1968.

[20] Dieter Forster. *Hydrodynamic Fluctuations, Broken Symmetry, And Correlation Functions*. Advanced Books Classics. Westview Press, Boulder, CO, 1995.

[21] J.T. Hynes and J.M. Deutch. Non-equilibrium problems - projection operator techniques. In H. Eyring, D. Henderson, and W. Jost, editors, *Physical Chemistry - An Advanced Treatise*, volume 11B, pages 729–836. Academic, 1975.

[22] Bobo Shi, Mithila V. Agnihotri, Si-Han Chen, Richie Black, and Sherwin J. Singer. Polarization charge: Theory and applications to aqueous interfaces. *J. Chem. Phys.*, 144(16):164702, 2016.

[23] Dieter Forster. *Hydrodynamic Fluctuations, Broken Symmetry, and Correlation Functions*. Number 47 in Frontiers in physics. W. A. Benjamin, Advanced Book Program, Reading, Mass, 1975.

[24] Lalith Perera and Max L. Berkowitz. Dynamics of ion solvation in a Stockmayer fluid. *J. Chem. Phys.*, 96(4):3092–3101, 1992.

[25] Lalith Perera and Max L. Berkowitz. Ultrafast solvation dynamics in a Stockmayer fluid. *J. Chem. Phys.*, 97(7):5253–5254, 1992.

[26] Lalith Perera and Max L. Berkowitz. Solvation dynamics in a Stockmayer fluid. In Lesser Blum and F. Bary Malik, editors, *Condensed Matter Theories*, volume 8, pages 461–483. Springer US, Boston, MA, 1993.

[27] M. Beleggia and M. De Graef. On the computation of the demagnetization tensor field for an arbitrary particle shape using a Fourier space approach. *J. Magn. Magn. Mater.*, 263(1):L1–L9, 2003.

[28] Marco Beleggia, Shakul Tandon, Yimei Zhu, and Marc De Graef. On the computation of the demagnetization tensor for particles of arbitrary shape. *J. Magn. Magn. Mater.*, 272-276:E1197–E1199, 2004.

Appendic 1. Surface of deformed droplet at constant volume

In polar coordinate, the radius of droplet can be expressed in terms of angles. And the function of radius can be decomposed into spherical harmonics.

$$r(\Omega) = r_0[1 + u(\Omega)] = r_0[1 + \sum_{\ell m} u_{\ell m} Y_{\ell m}(\Omega)] \tag{1}$$

Let $R(r, \Omega)$ be the difference between arbitrary radical distance from origin and the radius of droplet at this direction. The point is at the surface when $R(r, \Omega)$ is 0.

$$R(r, \Omega) = r - r(\Omega) = 0 \quad \text{indicates point on surface} \tag{2}$$

Thus, the unit vector orthogonal to the surface can be determined by taking the divergence of R and normalizing it.

$$\hat{\mathbf{n}}(\Omega) = \frac{\boldsymbol{\nabla} R}{|\boldsymbol{\nabla} R|} \quad \text{unit orthogonal vector on the surface} \tag{3}$$

The divergence and the normalization are done in spherical coordinate.

$$\boldsymbol{\nabla} = \hat{\mathbf{r}} \frac{\partial}{\partial r} + \hat{\boldsymbol{\theta}} \frac{1}{r} \frac{\partial}{\partial \theta} + \hat{\boldsymbol{\phi}} \frac{1}{r \sin\theta} \frac{\partial}{\partial \phi} \tag{4}$$

$$\boldsymbol{\nabla} R = \hat{\mathbf{r}} - \hat{\boldsymbol{\theta}} \frac{r_0}{r} u_\theta - \hat{\boldsymbol{\phi}} \frac{r_0}{r \sin\theta} u_\phi \tag{5}$$

$$\hat{\boldsymbol{n}}(\Omega) = \frac{\hat{\mathbf{r}} - \hat{\boldsymbol{\theta}} \xi u_\theta - \hat{\boldsymbol{\phi}} \frac{\xi}{\sin\theta} u_\phi}{\left(1 + (\xi u_\theta)^2 + (\frac{\xi u_\phi}{\sin\theta})^2\right)^{\frac{1}{2}}} \tag{6}$$

$$\xi = \frac{r_0}{r} \tag{7}$$

$$\tag{8}$$

First. the volume of droplet is determined using divergence theorem that $\int\limits_v \mathrm{d}\mathbf{r} \boldsymbol{\nabla} \cdot \boldsymbol{F} = \int\limits_s (\mathbf{F} \cdot \hat{\boldsymbol{n}}) \mathrm{d}A$.

In spherical coordinate,

$$\boldsymbol{\nabla} \cdot \boldsymbol{F} = \frac{1}{r^2 \sin\theta} \left[\sin\theta \frac{\partial}{\partial r} (r^2 \boldsymbol{F}_r) + r \frac{\partial}{\partial \theta} (\sin\theta \boldsymbol{F}_\theta) + r \frac{\partial}{\partial \phi} \frac{\partial \boldsymbol{F}_\phi}{\partial \phi} \right] \tag{9}$$

Let $\mathbf{F} = \frac{1}{3} r \hat{\mathbf{r}}$

$$\boldsymbol{\nabla} \cdot \mathbf{F} = \frac{1}{r^2 \sin\theta} \left[\sin\theta \frac{\partial}{\partial r} (\frac{1}{3} r^3) \right] = 1 \tag{10}$$

$$\tag{11}$$

$$\int_v \mathrm{d}\mathbf{r} \boldsymbol{\nabla} \cdot \boldsymbol{F} = \int_v \mathrm{d}\mathbf{r} = V \tag{12}$$

$$\int_v \mathrm{d}\mathbf{r} = \int_s \mathrm{d}A \, \frac{1}{3} r(\hat{\boldsymbol{n}} \cdot \hat{\boldsymbol{r}}) \tag{13}$$

$$= \int \mathrm{d}\Omega \, \frac{r^2}{(\hat{\boldsymbol{n}} \cdot \hat{\boldsymbol{r}})} \frac{r}{3} (\hat{\boldsymbol{n}} \cdot \hat{\boldsymbol{r}}) \tag{14}$$

$$= \int \mathrm{d}\Omega \, \frac{r^3}{3} \tag{15}$$

$$V = \int \mathrm{d}\Omega \frac{r_0^3 (1 + u(\Omega))^3}{3}$$

There is another way to understand this expression.

$$\mathrm{d}V = \text{volume of square pyramid} = \frac{1}{3} a^2 h \tag{16}$$

$$= \frac{1}{3} (r^2 \mathrm{d}\Omega) r = \mathrm{d}\Omega \frac{r^3(\Omega)}{3} \tag{17}$$

Insert $r = 1 + \sum_{\ell,m} u_{\ell,m} Y_{\ell,m}(\Omega)$ and expand.

$$V = \frac{r_0^3}{3} \int \mathrm{d}\Omega \left(1 + \sum_{\ell,m} u_{\ell,m} Y_{\ell,m}(\Omega) \right)^3 \tag{18}$$

$$= \frac{r_0^3}{3} \int \mathrm{d}\Omega \left[1 + 3 \sum_{\ell,m} u_{\ell,m} Y_{\ell,m}(\Omega) + 3 \sum_{\ell,m} \sum_{\ell',m'} u_{\ell,m} u^*_{\ell',m'} Y_{\ell,m}(\Omega) Y^*_{\ell',m'}(\Omega) + \mathcal{O}(u^3) \right] \tag{19}$$

$$= \frac{r_0^3}{3} \left[4\pi + 3(4\pi)^{\frac{1}{2}} u_{00} + 3 \sum_{\ell,m} |u_{\ell,m}|^2 + \mathcal{O}(u^3) \right] \tag{20}$$

$$= r_0^3 \left[\frac{4\pi}{3} + (4\pi)^{\frac{1}{2}} u_{00} + \sum_{\ell,m} |u_{\ell,m}|^2 \right] + \mathcal{O}(u^3) \tag{21}$$

$$= r_0^3 \left[\frac{4\pi}{3} + 4\pi u_0 + 4\pi u_0^2 + \sum_{\ell>0,m} |u_{\ell,m}|^2 \right] + \mathcal{O}(u^3) \qquad \text{let } u_0 = \frac{u_{00}}{(4\pi)^{\frac{1}{2}}} \tag{22}$$

$$= \frac{4\pi r_0^3}{3} \left[1 + 3u_0 + 3u_0^2 \right] + r_0^3 \sum_{\ell>0,m} |u_{\ell,m}|^2 + \mathcal{O}(u^3) \tag{23}$$

$$= \frac{4\pi r_0^3}{3} (1 + u_0)^3 + r_0^3 \sum_{\ell>0,m} |u_{\ell,m}|^2 + \mathcal{O}(u^3) \tag{24}$$

The advantage of this form is that one can keep $V = \frac{4\pi r_0^3}{3}$ by choosing u_0 to satisfy $\frac{4\pi r_0^3}{3}(1+u_0)^3 + r_0^3 \sum_{\ell>0,m} |u_{\ell,m}|^2 = \frac{4\pi r_0^3}{3}$.

$$(1+u_0)^3 = 1 - \frac{3}{4\pi} \sum_{\ell>0,m} |u_{\ell,m}|^2 \tag{25}$$

$$\tag{26}$$

Then, we integrate $\mathrm{d}A = \mathrm{d}\Omega \frac{r^2}{\hat{\boldsymbol{n}}\cdot\hat{\boldsymbol{r}}}$ to determine surface area of the droplet.

$$\hat{\boldsymbol{n}}\cdot\hat{\boldsymbol{r}} = \left(1 + (\xi u_\theta)^2 + (\frac{\xi u_\theta}{\sin\theta})^2\right)^{-\frac{1}{2}} \approx \left(1 + \frac{\xi^2}{2}(u_\theta^2 + \frac{u_\phi^2}{\sin^2\theta})\right)^{-1} \tag{27}$$

$$A = \int \mathrm{d}A = \int \mathrm{d}\Omega \frac{r^2}{\hat{\boldsymbol{n}}\cdot\hat{\boldsymbol{r}}} \tag{28}$$

$$= \int \mathrm{d}\Omega \left(r^2 + \frac{r_0^2}{2}(u_\theta^2 + \frac{u_\phi^2}{\sin^2\theta})\right) \tag{29}$$

Then, the integration is done separately for the first term and the second term:

$$\int \mathrm{d}\Omega (u_\theta^2 + \frac{u_\phi^2}{\sin^2\theta}) = \int \mathrm{d}\theta \int \mathrm{d}\phi \sin\theta \left(\frac{\partial u}{\partial\theta}\frac{\partial u}{\partial\theta} + \frac{1}{\sin^2\theta}\frac{\partial u}{\partial\phi}\frac{\partial u}{\partial\phi}\right) \text{ inte by part} \tag{30}$$

$$= \int \mathrm{d}\theta \int \mathrm{d}\phi\ u \left(-\frac{\partial}{\partial\theta}(\sin\theta\frac{\partial u}{\partial\theta}) - \frac{1}{\sin\theta}\frac{\partial^2 u}{\partial\phi^2}\right) \tag{31}$$

$$= \int \mathrm{d}\theta \int \mathrm{d}\phi\ \sin\theta u(-\frac{1}{\sin\theta}\frac{\partial}{\partial\theta}\sin\theta\frac{\partial}{\partial\theta} - \frac{1}{\sin^2\theta}\frac{\partial^2}{\partial^2\phi})u \tag{32}$$

$$= \int \mathrm{d}\Omega\ u\hat{\boldsymbol{L}}^2 u \qquad \text{where } \hat{\boldsymbol{L}}^2 Y_{\ell m} = \ell(\ell+1)Y_{\ell m} \tag{33}$$

$$= \int \mathrm{d}\Omega \sum_{\ell' m'} u^*_{\ell' m'} Y^*_{\ell' m'}(\Omega)\hat{\boldsymbol{L}}^2 \sum_{\ell m} u_{\ell m} Y_{\ell m}(\Omega) \tag{34}$$

$$= \sum_{\ell>0,m} |u_{\ell m}|^2 \ell(\ell+1) \tag{35}$$

$$\int \mathrm{d}\Omega\, r^2 = \int \mathrm{d}\Omega\, r_0^2(1+u)^2 \tag{36}$$

$$= \int \mathrm{d}\Omega\, r_0^2(1+2u+u^2) \tag{37}$$

$$= 4\pi r_0^2 + 2r_0^2 \int \mathrm{d}\Omega\, \underbrace{(4\pi)^{\frac{1}{2}} Y_{00}^*(\Omega)}_{=1} \sum_{\ell m} u_{\ell m} Y_{\ell m}(\Omega) + r_0^2 \int \mathrm{d}\Omega \sum_{\ell' m'} u_{\ell' m'}^* Y_{\ell' m'}^*(\Omega) \sum_{\ell m} u_{\ell m} Y_{\ell m}(\Omega) \tag{38}$$

$$= 4\pi r_0^2 + 2(4\pi)^{\frac{1}{2}} r_0^2 u_{00} + r_0^2 u_{00}^2 + r_0^2 \sum_{\ell>0,m} |u_{\ell,m}|^2 \qquad \text{let } u_0 = \frac{u_{00}}{(4\pi)^{\frac{1}{2}}} \tag{39}$$

$$= 4\pi r_0^2 + 8\pi r_0^2 u_0 + 4\pi r_0^2 u_0^2 + r_0^2 \sum_{\ell>0,m} |u_{\ell,m}|^2 \tag{40}$$

Now, we can write out the expression for area.

$$A = \int \mathrm{d}\Omega \left(r^2 + \frac{r_0^2}{2}(u_\theta^2 + \frac{u_\phi^2}{\sin^2\theta}) \right) \tag{41}$$

$$= 4\pi r_0^2(1+u_0)^2 + r_0^2 \sum_{\ell>0,m} |u_{\ell,m}|^2 + \frac{r_0^2}{2} \sum_{\ell>0,m} \ell(\ell+1)|u_{\ell,m}|^2 \tag{42}$$

$$= 4\pi r_0^2(1+u_0)^2 + r_0^2 \sum_{\ell>0,m} (1 + \frac{\ell(\ell+1)}{2})|u_{\ell,m}|^2 \tag{43}$$

We have the relation ship for constant volume that $(1+u_0)^3 = 1 - \frac{3}{4\pi}\sum_{\ell>0,m} |u_{\ell,m}|^2$. From this, we can have the expression for $(1+u_0)^2$.

$$(1+u_0)^2 = (1 - \frac{3}{4\pi} \sum_{\ell>0,m} |u_{\ell,m}|^2)^{\frac{2}{3}} \tag{44}$$

$$= 1 - \frac{1}{2\pi} \sum_{\ell>0,m} |u_{\ell,m}|^2 + \dots \tag{45}$$

Insert this, we have the expression of surface area of a droplet at constant volume.

$$A = 4\pi r_0^2(1+u_0)^2 + r_0^2 \sum_{\ell>0,m} (1 + \frac{\ell(\ell+1)}{2})|u_{\ell,m}|^2 \tag{46}$$

$$= 4\pi r_0^2(1 - \frac{1}{2\pi} \sum_{\ell>0,m} |u_{\ell,m}|^2) + r_0^2 \sum_{\ell>0,m} (1 + \frac{\ell(\ell+1)}{2})|u_{\ell,m}|^2 \tag{47}$$

$$= 4\pi r_0^2 + r_0^2 \sum_{\ell>0,m} (\frac{\ell(\ell+1)}{2} - 1)|u_{\ell,m}|^2 \tag{48}$$

$$= 4\pi r_0^2 + \frac{r_0^2}{2} \sum_{\ell>0,m} (\ell(\ell+1) - 2)|u_{\ell,m}|^2 \tag{49}$$

$$= 4\pi r_0^2 + \frac{r_0^2}{2} \sum_{\ell>0,m} (\ell+2)(\ell-1)|u_{\ell,m}|^2 \tag{50}$$

$$\tag{51}$$

Appendix 1. Hamiltonian of infinite slab and uniformly polarized sphere

(1) Infinite slab.

$$E_{pol} = \int_V \left[\frac{P^2}{2\varepsilon_0(\varepsilon_r - 1)} - \vec{E}_0 \cdot \vec{P} + E_{columbs} \right]$$

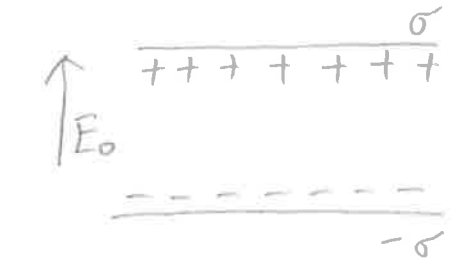

The boundary charge density caused by polarization is $\sigma = \vec{P} \cdot \hat{n}$ $\hat{n}$ is unit vector perpendicular to the surface.

We need to include the charge-charge repulsion and attraction in the total energy.

① Between surface — attraction

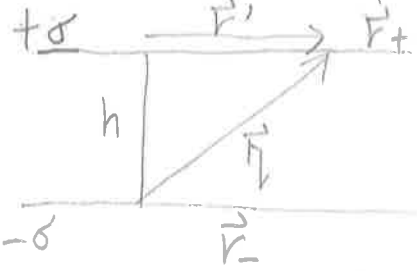

$$E_{attra} = \frac{1}{4\pi\varepsilon_0} \int_{s+} da_+ \int_{s-} da_- \frac{-\sigma^2}{|\vec{r}_+ - \vec{r}_-|}$$

$$= \frac{1}{4\pi\varepsilon_0} \int_0^{2\pi} d\theta_1 \int_0^{R\to\infty} r_1 \, dr_1$$

since it's symmetric $\int_0^{2\pi} d\theta_2 \int_0^{R\to\infty} r_2 \, dr_2 \frac{-\sigma^2}{|\vec{r}_1 - \vec{r}_2|}$

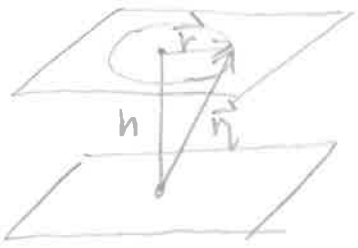

$$= \frac{1}{4\pi\varepsilon_0} a \int_0^{2\pi} d\theta \int_0^{R\to\infty} dr \frac{-\sigma^2}{\sqrt{h^2 + r^2}}$$

$$= \frac{-\sigma^2}{4\pi\varepsilon_0} a \, 2\pi \sqrt{h^2 + r^2} \Big|_0^{R\to\infty}$$

$$= -a \frac{\sigma^2}{2\varepsilon_0} \left(\sqrt{h^2 + R^2} - h \right) \Big|_{R\to\infty}$$

② Within same surface —— repulsion

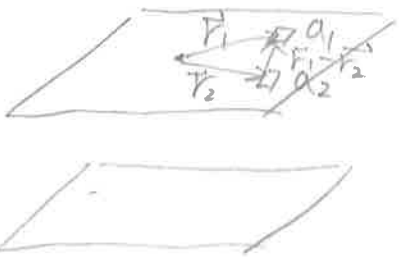

$$E_{rep} = 2 \times \frac{1}{4\pi\varepsilon_0} \times \frac{1}{2} \int da_1 \int da_2 \frac{\sigma^2}{|\vec{r}_1 - \vec{r}_2|}$$

$$= \frac{\sigma^2}{4\pi\varepsilon_0} a \int_0^{2\pi} d\theta \int_0^{R\to\infty} r\,dr \frac{1}{\sqrt{r^2}}$$

$$= a \frac{\sigma^2}{2\varepsilon_0} R\Big|_{R\to\infty}$$

$$E_{columbs} = E_{attra} + E_{repul}$$

$$= \lim_{R\to\infty} a \frac{\sigma^2}{2\varepsilon_0} \left[-\sqrt{h^2+R^2} + h + R \right]$$

$$= \lim_{R\to\infty} a \frac{\sigma^2}{2\varepsilon_0} R \left[1 - \sqrt{1+\left(\frac{h}{R}\right)^2} + \frac{h}{R} \right]$$

$$= \lim_{R\to\infty} a \frac{\sigma^2}{2\varepsilon_0} R \left[1 - \left(1 + \frac{1}{2}\left(\frac{h}{R}\right)^2 + \dots\right) + h \right]$$ Taylor expansion

$$= \frac{\sigma^2}{2\varepsilon_0} ah$$

$$= \frac{P^2}{2\varepsilon_0} V \qquad V = ah$$

Thus, $$U_{tot} = E_{pol} = V\left[\frac{P^2}{2\varepsilon_0(\varepsilon_r - 1)} - \varepsilon_0 P + \frac{P^2}{2\varepsilon_0}\right]$$

$$= V\left[\frac{P^2}{2\varepsilon_0}\frac{\varepsilon_r}{\varepsilon_r - 1} - \varepsilon_0 P\right]$$

(11) Sphere

Same as infinite slab, there is a term of Coulomb potential due to the boundary charge. It's assumed that polarization is uniform.

$$U_{coul} = \frac{1}{2} r^4 \int d\theta \int d\phi \int d\theta' \int d\phi' \sin\theta \sin\theta' \frac{(P\cos\theta)(P\cos\theta')}{4\pi\epsilon_0 |\vec{r} - \vec{r}'|}$$

$$= \frac{1}{2} \frac{r^4 P^2}{4\pi\epsilon_0} \int d\theta \int d\phi \int d\theta' \int d\phi' \sin\theta \sin\theta' \; C_{10}(\theta, \phi) \, C_{10}^*(\theta', \phi') \frac{1}{|\vec{r} - \vec{r}'|}$$

$$\cos\theta = C_{10}$$

$$\frac{1}{|\vec{r} - \vec{r}'|} = \sum_{l,m} \frac{r_<^l}{r_>^{l+1}} C_{lm}^*(\theta, \phi) \, C_{lm}(\theta', \phi')$$

$r_> = \max(r, r')$ $\quad r_< = \min(r, r')$

$C_{lm}(\theta, \phi)$ is orthoganal set.

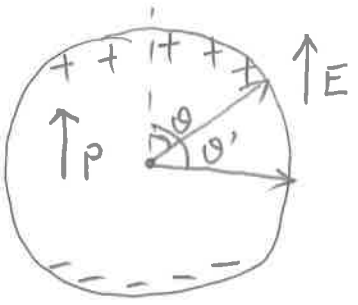

$\sigma = P\cos\theta$

Thus,

$$U_{coul} = \frac{1}{2} \frac{r^4 P^2}{4\pi\epsilon_0} \frac{1}{r} \left[\int d\theta \int d\phi \sin\theta \cos^2\theta \right]^2$$

$$= \frac{1}{2} \frac{r^4 P^2}{4\pi\epsilon_0} \frac{1}{r} \left(\frac{4}{3}\pi \right)^2$$

$$= \left(\frac{4}{3}\pi r^3 \right) \left(\frac{P^2}{6\epsilon_0} \right)$$

$$= V \frac{P^2}{6\epsilon_0}$$

The total energy is:

$$U = V \left[\frac{P^2}{2\epsilon_0(\epsilon_r - 1)} - E_0 P + \frac{P^2}{6\epsilon_0} \right]$$

$$= V \left[\frac{P^2}{2\epsilon_0} \frac{\epsilon_r + 2}{3(\epsilon_r - 1)} - E_0 P \right]$$

Appendix . Total energy of a slightly deformed droplet in uniform electric field.

$$U_{coul} = \frac{1}{2}\int d^2\vec{r}_1 \int d^2\vec{r}_2 \frac{\sigma_{pol}(\vec{r}_1)\,\sigma_{pol}(\vec{r}_2)}{4\pi\varepsilon_0 |\vec{r}_1 - \vec{r}_2|}$$

$$= \frac{1}{2}\int d^2\vec{r}_1 \int d^2\vec{r}_1' \int d^2\vec{r}_2 \int d^2\vec{r}_2' \frac{\sigma(\vec{r}_1')\,\delta(\vec{r}_1 - \vec{r}_1')\,\sigma(\vec{r}_2')\,\delta(\vec{r}_2 - \vec{r}_2')}{4\pi\varepsilon_0 |\vec{r}_1 - \vec{r}_2|}$$

$$= \frac{1}{2}\frac{1}{4\pi\varepsilon_0}\int d^2\vec{r}_1 \int d^2\vec{r}_1' \int dk_1 \int d^2\vec{r}_2 \int d^2\vec{r}_2' \int dk_2$$

$$\sigma(\vec{r}_1')\frac{e^{ik(\vec{r}_1' - \vec{r}_1)}}{(2\pi)^3}\frac{1}{4\pi\varepsilon_0|\vec{r}_1 - \vec{r}_2|}\sigma(\vec{r}_2')\frac{e^{ik(\vec{r}_2 - \vec{r}_2')}}{(2\pi)^3}$$

$$= \frac{1}{2}\frac{1}{4\pi\varepsilon_0}\frac{1}{(2\pi)^6}\int dk_1 \int dk_2\, \sigma^*(k_1)\, f(k_1, k_2)\, \sigma(k_2)$$

Where

$$\sigma(\vec{k}) = \int d\vec{r}\; e^{-i\vec{k}\cdot\vec{r}}\,\sigma(\vec{r})$$

$$\left(\sigma(\vec{r}) = \frac{1}{(2\pi)^3}\int d\vec{k}\; e^{i\vec{k}\cdot\vec{r}}\,\sigma(\vec{k})\right)$$

$$f(\vec{k}_1, \vec{k}_2) = \int d\vec{r}_1 \int d\vec{r}_2\; e^{-i\vec{k}_1\cdot\vec{r}_1 + i\vec{k}_2\cdot\vec{r}_2}\frac{1}{|\vec{r}_1 - \vec{r}_2|}$$

$$f(\vec{k}_1, \vec{k}_2) = \int d\vec{r}_1 \int d\vec{r}_2\; e^{-i\vec{k}_1\cdot\vec{r}_1}\, e^{i\vec{k}_2\cdot\vec{r}_2}\frac{1}{|r_1 - r_2|}$$

$$= \int d\vec{r}_1 \int d\vec{r}_2\; e^{-i\vec{k}_1\cdot(\vec{r}_1 - \vec{r}_2)}\, e^{i(\vec{k}_2 - \vec{k}_1)\cdot\vec{r}_2}\frac{1}{|\vec{r}_1 - \vec{r}_2|}$$

Change variable to $\vec{r}_1 - \vec{r}_2 = \vec{r}$ and $\vec{r}_2$

$$= \int d\vec{r}_2\; e^{i(\vec{k}_2 - \vec{k}_1)\cdot\vec{r}_2}\int d\vec{r}\; e^{-i\vec{k}_1\cdot\vec{r}}\frac{1}{|r|}$$

$$= (2\pi)^3\,\delta(\vec{k}_1 - \vec{k}_2)\int d\Omega \int_0^\infty dr\, r^2\, e^{-ik_1 r\cos\theta}\frac{1}{r}$$

$$= (2\pi)^4\,\delta(\vec{k}_1 - \vec{k}_2)\int_0^\infty dr\,\frac{e^{-ik_1 r} - e^{ik_1 r}}{-ik_1}$$

$$= (2\pi)^4 \delta(\vec{k}_1 - \vec{k}_2) \lim_{\epsilon \to 0} \int_0^\infty dr \frac{2\sin(k_1 r) e^{-\epsilon r}}{k_1}$$

$$= (2\pi)^4 \delta(\vec{k}_1 - \vec{k}_2) \lim_{\epsilon \to 0} \frac{2k_1}{\epsilon^2 + k_1^2} \frac{1}{k_1^2}$$

$$= 2(2\pi)^4 \delta(\vec{k}_1 - \vec{k}_2) \frac{1}{k_1^2}$$

$$U_{coul} = \frac{1}{2(2\pi)^6 4\pi\epsilon_0} \int d\vec{k}_1 \int d\vec{k}_2 \, \sigma^*(\vec{k}_1) \sigma(\vec{k}_2) \, 2(2\pi)^4 \delta(\vec{k}_1 - \vec{k}_2) \frac{1}{k_1^2}$$

$$= \frac{1}{2(2\pi)^6 4\pi\epsilon_0} \int d\vec{k}_1 |\sigma(\vec{k}_1)|^2 \, 2(2\pi)^4 \frac{1}{k_1^2}$$

$$= \frac{1}{(2\pi)^2 4\pi\epsilon_0} \int d\vec{k} \, |\sigma(\vec{k})|^2 \frac{1}{k^2}$$

Now, we want to have the $\sigma(\vec{k})$.

$$\vec{P}(\vec{r}) = -\vec{\nabla}\sigma(\vec{r}) = \frac{1}{(2\pi)^3} \int d\vec{k} \, e^{i\vec{k}\cdot\vec{r}} \left[-i\vec{k}\,\sigma(\vec{k})\right]$$

$$= \frac{1}{(2\pi)^3} \int d\vec{k} \, e^{i\vec{k}\cdot\vec{r}} \, \vec{P}(\vec{k})$$

$$\vec{P}(\vec{k}) = -i\vec{k}\,\sigma(\vec{k})$$

$$\sigma(\vec{k}) = i\vec{k}\cdot\vec{P}(\vec{k}) = ik\hat{k}\cdot\vec{P}(\vec{k})$$

Thus,

$$U_{coul} = \frac{1}{(2\pi)^2 4\pi\epsilon_0} \int d\vec{k} \, |\hat{k}\cdot\vec{P}(\vec{k})|^2$$

Now, we want to have $\vec{P}(k)$ for deformed droplet that $r(\Omega) = r_0(1+u(\Omega)) = r_0\left(1+\sum_{l,m} u_{lm} Y_l^m(\Omega)\right)$.

Assume constant polarization

$$\vec{P}_0(\vec{k}) = \vec{P}_0 \int_V d^3\vec{r}\, e^{-i\vec{k}\cdot\vec{r}}$$

$$= \vec{P}_0 \int d\Omega \int_0^{r_0(1+u(\Omega))} r^2 dr\, e^{-ikr\cos\theta}$$

$$= \vec{P}_0 \int d\Omega \frac{2i + e^{-ik\cos\theta\, r(\Omega)}\left(-2i + r(\Omega)k\cos\theta\,(2 + i r(\Omega) k\cos\theta)\right)}{(k\cos\theta)^3}$$

Expand $e^{r(\Omega)} = e^{1+u(\Omega)}$ since $u(\Omega)$ is very small.

$$\vec{P}_0(\vec{k}) = \vec{P}_0 \vec{r}_0^{\,3} \Big\{ \int d\Omega \frac{\sin(kr_0) - kr_0\cos(kr_0)}{(kr_0)^3} \quad ① \Big\} \text{ main contribution}$$

$$+ \int d\Omega\, e^{ikr_0\cos\theta}\, u(\Omega) \quad ②$$

$$+ \int d\Omega\, e^{ikr_0\cos\theta}\left(1 - \tfrac{1}{2} ikr_0\cos\theta\right) u^2(\Omega)$$

$$+ \mathcal{O}(u^3) \Big\}.$$

Let's deal ② term.

$$e^{i\vec{k}\cdot\hat{r} r_0} = \sum_l (2l+1) i^l j_l(kr_0) \sum_q C_{lq}(\Omega') C_{lq}^*(\Omega)$$

(j_l: spherical Bessel functions)

$$C_{lm}(\Omega) = \left(\frac{4\pi}{2l+1}\right)^{\frac{1}{2}} Y_l^m(\Omega)$$

Ω = angle between $\vec{r}$ and $\vec{P}_0$

Ω' = angle between $\vec{k}$ and $\vec{P}_0$

$$\int d\Omega\, e^{i\vec{k}\cdot\hat{r} r_0} u(\Omega)$$

$$= \sum_{lq} \sum_{lm} (2l+1) i^l j_l(kr_0) \left(\frac{4\pi}{2l+1}\right) Y_{lm}(\Omega') u_{lm} \int d\Omega\, Y_{lq}(\Omega) Y_{lm}^*(\Omega)$$

$$= 4\pi \sum_{lm} i^l j_l(kr_0) Y_l^m(\Omega') u_{lm}$$

Thus, $\vec{P}(\vec{k}) = \vec{P}_0 r_0^3 \left\{ 4\pi \frac{\sin(kr_0) - kr_0\cos(kr_0)}{(kr_0)^3} \right.$

$$\left. + 4\pi \sum_{lm} i^l j_l(kr_0) Y_l^m(\Omega') u_{lm} \right\} + \vartheta$$

$$U_{coul} = \frac{1}{(2\pi)^2 4\pi\epsilon_0} \int d\vec{k} \left| \cos\theta\, P_0 r_0^3 \left\{ 4\pi \frac{\sin(kr_0) - kr_0\cos(kr_0)}{(kr_0)^3} \right. \right.$$

$$\left. \left. + 4\pi \sum_{lm} i^l j_l(kr_0) Y_l^m(\Omega') u_{lm} \right\} \right|^2$$

$$= \frac{1}{(2\pi)^2 4\pi\epsilon_0} \int d\vec{k}\ \cos^2\theta\, P_0^2 r_0^6 \left\{ \left(4\pi \frac{\sin(kr_0) - kr_0\cos(kr_0)}{(kr_0)^3} \right)^2 \right.$$

$$+ 4\pi \frac{\sin(kr_0) - kr_0\cos(kr_0)}{(kr_0)^3} 4\pi \sum_{lm} j_l(kr_0) \left[i^l Y_l^m(\theta,\phi) u_{lm} \right.$$

$$\left. + (-i)^l Y_l^{m*}(\theta,\phi) u_{lm}^* \right]$$

$$\left. + \left| 4\pi \sum i^l j_l(kr_0) Y_l^m(\theta,\phi) u_{lm} \right|^2 \right\}$$

$$\frac{4\pi}{(kr_0)^3} \left(\sin(kr_0) - kr\cos(kr_0) \right) = \frac{4\pi}{kr_0} \left[\frac{\sin(kr_0)}{(kr_0)^2} - \frac{\cos(kr_0)}{kr_0} \right]$$

$$= \frac{4\pi}{kr_0} j_1(kr_0)$$

$z = kr_0 \quad dz = r_0 dk$

$$\bar{E}_{pol} = \frac{r_0^6 P_0^2 (4\pi)^2}{(2\pi)^2 4\pi\epsilon_0} \left\{ \int d\Omega \cos^2\theta \frac{1}{r_0^3} \int_0^\infty dz\, j_1(z) j_1(z) \right.$$

$$+ \sum_{lm} u_{lm} \int d\Omega \cos^2\theta Y_{lm}(\theta,\phi)\, i^l \int_0^\infty dk\, k^2 \frac{j_1(kr_0)}{kr_0} j_l(kr_0)$$

$$+ \sum_{lm} u_{lm}^* \int d\Omega \cos^2\theta Y_{lm}^*(\theta,\phi)(-i)^l \int_0^\infty dk\, k^2 \frac{j_1(kr_0)}{kr_0} j_l(kr_0)$$

$$\left. + \cdots \right\}$$

$$\int d\Omega \cos^2\theta = \frac{4}{3}\pi \qquad \int_0^\infty dz\, j_1(z)^2 = \frac{\pi}{6}$$

$$\int d\Omega \cos^2\theta Y_l^m(\theta,\phi) = \int d\Omega\, \pi^{\frac{1}{2}} \left[\frac{2}{3} Y_{00}(\theta,\phi) + \frac{4}{3}\frac{1}{\sqrt{5}} Y_{20}(\theta,\phi) \right]$$

Y_{lm}

$$= \frac{2}{3}\pi^{\frac{1}{2}} \left[\delta_{l0}\delta_{m0} + \frac{2}{\sqrt{5}} \delta_{l2}\delta_{m0} \right]$$

$$\int_0^\infty dk\, k^2 \frac{j_1(kr_0)}{kr_0} j_l(kr_0) = \frac{1}{r_0^3} \int_0^\infty dz\, z\, j_1(z) j_l(z)$$

$$= \frac{1}{r_0^3}\frac{\pi}{4} \quad \text{if } l=0 \text{ or } l=2$$

$$u_{pol} = \frac{r_0^3 P_0^2}{\pi\epsilon_0} \left\{ 2\pi \frac{2}{3}\frac{\pi}{6} - 2\frac{2}{3}\pi^{\frac{1}{2}} \left(u_{00} + \frac{2}{\sqrt{5}} u_{20}\right)\frac{\pi}{4} + \mathcal{O}(u_{lm}^2) \right\}$$

$$= \frac{4\pi r_0^3 P_0^2}{3\epsilon_0} \left\{ \frac{1}{6} + \frac{1}{4\sqrt{\pi}} u_{00} + \frac{1}{2\sqrt{5\pi}} u_{20} + \mathcal{O} \right\}$$

$$= \frac{4\pi r_0^3 P_0^2}{3\epsilon_0} \left\{ \frac{1}{6} - \frac{1}{2\sqrt{5\pi}} u_{20} + \mathcal{O} \right\}$$

$$E_{tot} = \gamma A + \frac{4}{3}\pi r_0^3 \left\{ \frac{P_0^2}{3\epsilon_0(\epsilon_r - 1)} - E_0 P_0 + P_0^2 \left(\frac{1}{6} - \frac{1}{2\sqrt{5\pi}} u_{20} + \cdots \right) \right\}$$

For a droplet with constant volume $\frac{4}{3}\pi r_0^3$,

$$A = 4\pi r_0^2 + \frac{r_0^2}{2} \sum_{l>0, m} (l+2)(l-1) |u_{lm}|^2$$

$$E_{tot} = \gamma \left\{ 4\pi r_0^2 + \frac{r_0^2}{2} \sum_{l \geq 2} (l+2)(l-1) |u_{lm}|^2 \right\}$$

$$+ \frac{4\pi r_0^3}{3\epsilon_0} \left\{ \frac{P_0^2}{2(\epsilon_r - 1)} - \epsilon_0 E_0 P_0 + P_0^2 \left(\frac{1}{6} - \frac{1}{2\sqrt{5\pi}} u_{20} + \cdots \right) \right\}$$

$$= \gamma \left\{ 4\pi r_0^2 + \frac{r_0^2}{2} \sum_{l \geq 2} (l+2)(l-1) |u_{lm}|^2 \right\}$$

$$+ \frac{4\pi r_0^3}{3\epsilon_0} \left\{ -\epsilon_0 E_0 P_0 + \frac{P_0^2}{2} \left(\frac{\epsilon_r + 2}{3(\epsilon_r - 1)} - \frac{1}{\sqrt{5\pi}} u_{20} + \cdots \right) \right\}$$